Chapter 5

Types of Cavitation: BUBBLE CAVITATION

Objective: *Description of the appearance and behavior of bubble cavitation*

When observed in white light cavitation is only a hazy blur on a surface. As is often the case (see the work of Parsons in chapter 2) good observations in an adequate test setup opened new perspectives. This was the case with the first high speed observations in 1948 by Knapp and Hollander [26]. They investigated a *headform*, which is a cylindrical body with a certain contour. The contour they investigated was a *hemispere*, which at that time was used as a standard body for the comparison of cavitation and cavitation inception in various facilities.

Knapp and Hollander observed cavitation in the low pressure region of such a headform. Instead of stroboscopic illumination, which resulted in a series of unrelated observations of bubble cavitation (Fig. 5.1 [19]), they applied a rotating mirror in combination with a film camera to observe the cavitation. This was the beginning of high speed observations. As a result they could observe the growth and collapse of bubble cavitation on the headform (Fig 5.2).

This made it possible to plot the bubble radius over time. Knapp and Hollander showed that the bubble growth could accurately be described by the Raleigh Plesset equation (eq.4.6), as shown in Fig. 5.3.

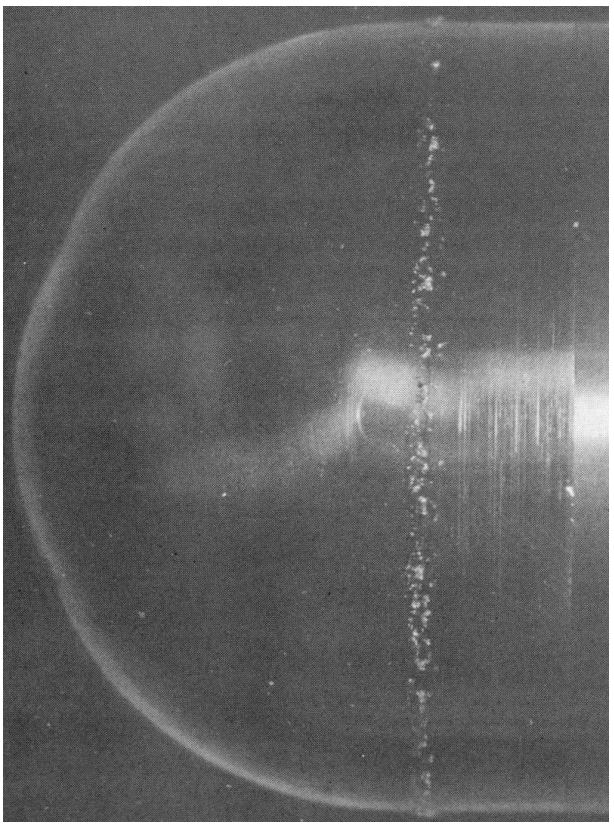

Figure 5.1: Observations of Bubble Cavitation on a Headform. From [27]

When a nucleus grows into a bubble cavity the effect of the surface tension becomes negligible, so the bubble motion is governed by inertia. From Fig. 5.3 it can be seen that the overshoot of the bubble radius is consid-

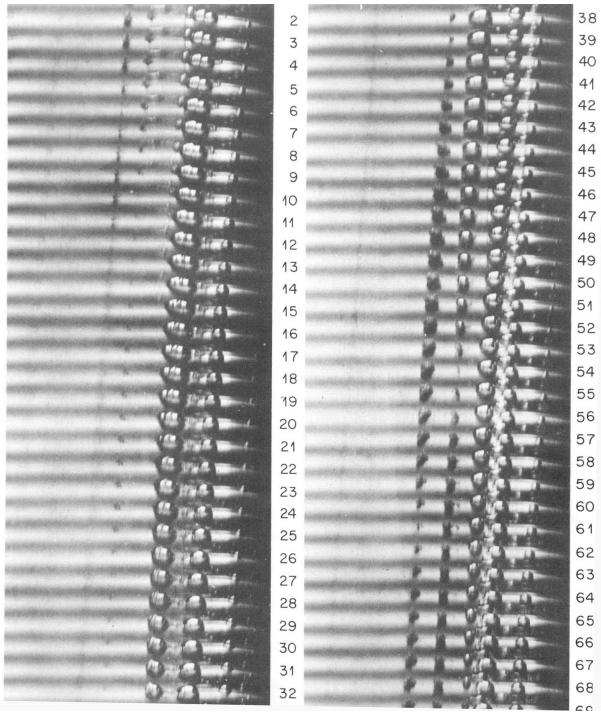

Figure 5.2: High Speed Observations of Bubble Cavitation on a Headform. From [27]

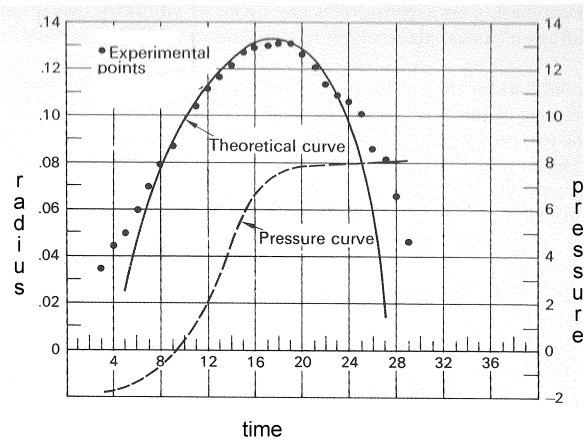

Figure 5.3: Pressure and Bubble Response on a Hemispherical Headform

erable: the bubble reaches its maximum size when the pressure has already returned to the undisturbed pressure. The potential energy stored in the cavitation bubble is then converted into kinetic energy during the collapse phase. This was used by Raleigh to formulate in 1917 the collapse time of a bubble for a bubble with radius R_{max} and zero internal pressure (the vapor pressure is neglected, as well as the gas pressure and the surface tension):

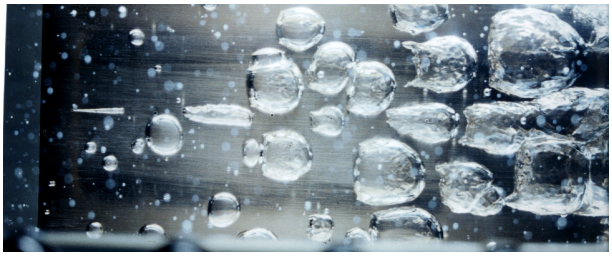

Figure 5.4: Bubble Cavitation on a 2D foil

$$t = 0.91468 R_{max} \sqrt{\frac{\rho_w}{p_\infty}} \qquad (5.1)$$

The collapse time is generally very short. To get an idea: a cavitation bubble of 1 cm (0.01m) in radius which returns from the vapor pressure to atmospheric pressure ($p_\infty = 10^5 Pa$) takes only 1 millisecond to collapse! However, on a propeller blade of a model propeller at a fluid velocity of 10 m/sec this bubble will still move over 1 cm in distance during collapse, which is not negligible.

5.1 Bubble cavitation on a foil

On a two-dimensional foil the appearance of bubble cavitation can be observed in more detail. An example is Fig. 5.4.

In this situation the bubble cavities reach a significant size, which indicates that the nuclei content is not very high. It is also observed that the bubble cavities are no longer spherical. The streamwise pressure gradient causes a flat part on the bubbles. Although not seen

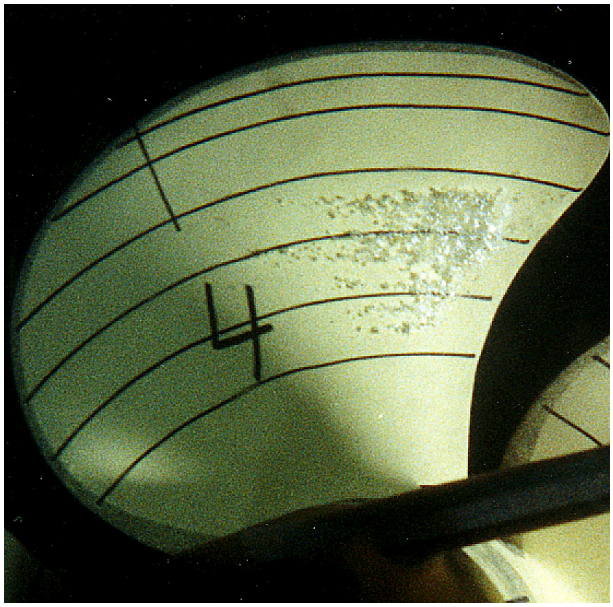

Figure 5.5: Bubble Cavitation on a Propeller Model

in this picture, the bubbles will also attach to the surface and become non-sperical near the wall. The shear in the boundary layer causes a distortion of the cavity, which is apparent by the small twin "horns" which are directed upstream. At inception this deformation is not yet present, so for nuclei the assumption of spherical bubbles can be used.

5.2 Bubble cavitation on a model propeller

The natural type of cavitation following from expanding nuclei is bubble cavitation. When the nuclei grow to visible size and larger due to a low external pressure the gas content inside the bubble as well as the surface pressure on the bubble wall become insignificant and the pressure inside the bubble will be close to the vapor pressure. Fig. 5.5 shows bubble cavitation on the model of a ship propeller.

The origin of each bubble in Fig.5.5is a nucleus which grows with decreasing pressure. It should be kept in mind that when the bubbles

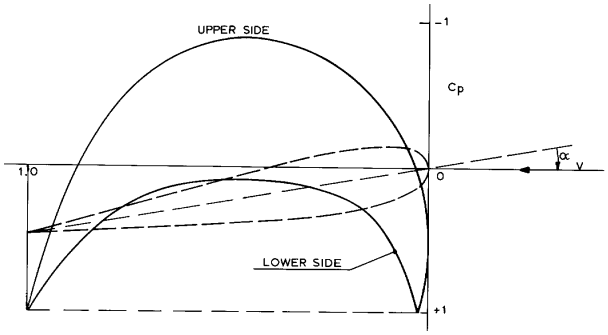

Figure 5.6: Schematical Pressure Distribution on a Foil with Bubble Cavitation

become visible the partial pressure of the gas is already negligible and that the bubbles can be considered as filled with vapor at the vapor pressure. The pressure distribution on the blade sections of Fig.5.5 is such that there is a more or less gradual decrease of the pressure from the leading edge, with a minimum pressure between 30 and 80 percent of the chord, after which the pressure increases again to the undisturbed pressure, as sketched in Fig.5.6. The essential element of the formation of bubble cavitation is that the bubbles have time to grow without causing flow separation. The result is that the cavitation bubbles move with the flow. Therefore this type of cavitation is also called traveling bubble cavitation.

5.2.1 The extent of bubble cavitation

In Fig.5.5 it can be seen that the maximum size of the bubbles occurs at the trailing edge of the cavitating region. This location is downstream of the minimum pressure location because of the overshoot of the bubble radius and because of the interaction between the bubbles and the pressure distribution. After reaching the maximum size the bubbles are in a much higher pressure than equilibrium and a rapid collapse will follow. The chordwise extent of bubble cavitation is therefore greater than the area on the propeller at which the pressure is

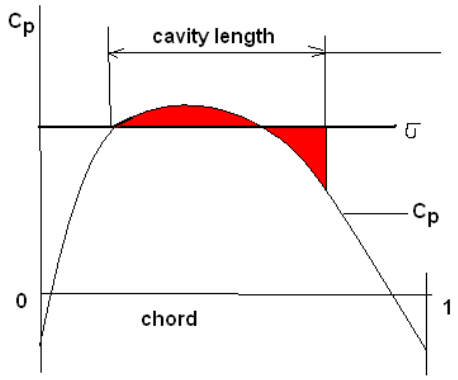

Figure 5.7: Estimate of cavity length from the non-cavitating pressure distribution

below the vapor pressure! Limited cavitation has no drastic effect on the lift of a section. Using this a very rough estimate of the cavity extent can be found from the non-cavitating pressure distribution and the cavitation index. The pressure increase due to cavitation has to be compensated by a pressure decrease downstream, as shown by the red area in Fig. 5.7.

5.2.2 Relation of bubble cavitation with nuclei distribution

When a nucleus is in a region with a pressure lower than the vapor pressure, it will grow indefinitely. The mechanism to stop the growth is interaction between the bubble and the surrounding pressure field. The bubble growth increases the surrounding pressure and the result will be that the pressure around the bubble cavities rises until the vapor pressure is reached. As can be seen in Fig.5.5 the bubbles coalesce and individual bubbles cannot be distinguished anymore. Efforts to relate the nuclei density with the amount of cavitation bubbles are fruitless, because when the largest nuclei begin to affect the flow, the smaller will not grow anymore or even do not become unstable. The number of cavitation bubbles in bubble cavitation only reflects a band of the largest available nuclei. The width of that band is very difficult to determine.

5.3 Inception of bubble cavitation

The definition of inception of bubble cavitation has been discussed in detail in section 4. The conditions of the flow should be such that no gaseous cavitation is present by limiting the number and size of large nuclei in the inflow. In general there is more risk of a lack of nuclei, so that inception is detected too late. The fact that bubble cavitation has the reputation of being erosive may be due to the fact that it was detected too late at model scale.

A lack of nuclei density can be detected by observing the size of nuclei at cavitation inception. When nuclei are lacking the minimum pressure on the blade sections will be below the vapor pressure. When a single nucleus becomes unstable at that pressure it will grow rapidly and relatively unrestricted to a significant size (Fig. 4.5). Then it can be concluded that the inception pressure is below the vapor pressure. When the cavitation bubbles are small at inception there are enough nuclei present. That does not yet mean that the nuclei are large enough. The inception pressure of small nuclei may still be much lower than the vapor pressure, even when there are enough of them. However, in general the nuclei density will decrease with increasing nuclei size. So at inception there will be less bubbles than at a lower pressure. Proper inception is called when a few bubbles are visible just be-

fore inception and when the size of these bubbles is small.

5.4 The appearance of bubble cavitation

When large nuclei are scarce the amount of bubble cavities is small. In that case the individual cavities can grow to a large size until their effect on the pressure is felt. When many nuclei are present the same effect on the pressure is felt by many smaller nuclei and the maximum size of the cavities will thus remain smaller. In the first three figures of Fig.5.8 the amount of nuclei in the incoming flow is gradually increased. The observations are made in uniform inflow and the increase in nuclei content is obtained by electrolysis upstream of the propeller ([34].

The number of bubble cavities increases when nuclei are generated, but the maximum size is not so much different yet. When the (local) nuclei density is drastically increased, as is the case in the fourth picture of Fig. 5.8, the maximum size decreases. The increase in nuclei in this fourth picture has been obtained by leading edge roughness, as will be discussed later. The change in appearence of bubble cavitation with incresing number of nuclei can be extrapolated to full scale. At full scale an abundance of nuclei is available and the maximum size of the individual bubble cavities will be small. An observation of bubbly cavitation at full scale is given in Fig. 5.9 and the full scale bubble cavitation is a fine mist of very small cavitation bubbles.

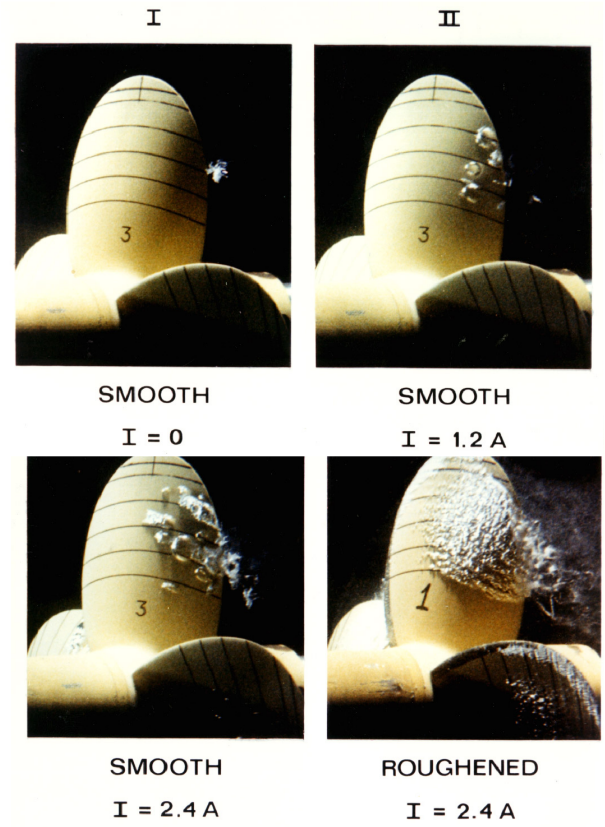

Figure 5.8: Bubble cavitation with increasing nuclei content

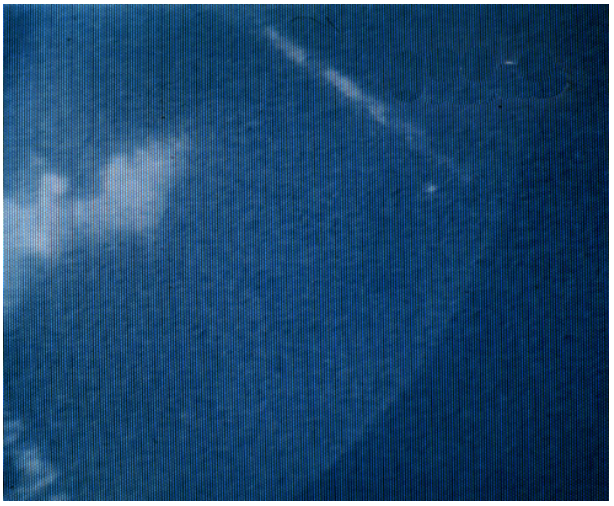

Figure 5.9: Bubble Cavitation on a Propeller at Full Scale

5.5 Effects of leading edge roughness on inception of bubble cavitation

Inception of bubble cavitation is controlled by the nuclei spectrum in the bulk flow. However, roughness elements may also serve as nuclei generators. This is because cavitation has the property of absorbing dissolved gases and after implosion these gases remain as free gas nuclei nuclei in the flow, as can be observed in Fig. 8.8on page 63. Downstream of the spots a stream of gas bubbles can sometimes be observed. (In fact such a bubble is a tiny sheet cavity as will be discussed in chapter 6). Experience is that even when the roughness elements are in regions with a mean pressure higher than the vapor pressure, still nuclei are generated by roughness. The precise mechanism and required conditions are not yet clear, but it seems that micro cavitation occurs in low pressure locations in the roughened region, as sketched in Fig. 5.10. Since cavitation causes diffusion of dissolved gas into the micro-cavity, a small gas bubble is created by the micro cavity. In this mechanism nuclei in the bulk flow are still necessary for inception of micro-cavitation, but the size of the nuclei required is much smaller then for bubble cavitation in the free flow.
A mechanism which may enhance the presence of nuclei near the turbulent boundary layer is turbulent mixing, which may reduce the effect of bubble screening. These phenomena still have to be investigated further. The effects of leading edge roughness on bubble cavitation can be very significant, as shown in Fig. 5.8. The first three pictures show the effect of electrolysis, so of an increasing amount and size of bulk nuclei. The last picture shows the additional effect of leading edge roughness. In this case the leading edge pressure is above the vapor pressure and there is no cavitation on the

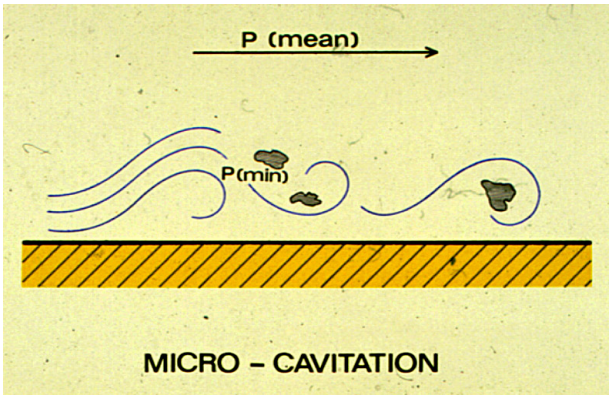

Figure 5.10: Generation of nuclei in a boundary layer with roughness

leading edge roughness. Still the roughness particles generate an abundant amount of nuclei which alter the appearance of the bubble cavitation at midchord completely.

5.6 Erosiveness of Bubble Cavitation

The question is if it is necessary to scale the amount of bubbles in model tests. A reason would be to scale the erosiveness properly. But erosiveness is not measured up to now, apart from techniques such as the paint technique (see chapter **??**. The amount of energy in the collapse of a single bubble and of a spherical cloud of bubbles with the same radius is about the same. So even when the number of bubbles in bubble cavitation is different from full scale, the erosion properties may still scale properly. The noise properties are more difficult to scale because of interaction between the bubbles.

Bubble cavitation has a longstanding reputation of being erosive in all cases and consequently propellers are generally designed with a certain margin against bubble cavitation. A consequence of that is that it is difficult to find full scale observations

of bubble cavitation.however, the reason why bubble cavitation is more erosive than e.g. sheet cavitation is not obvious. Navy propellers designed for maximum inception speed often have bubble cavitation at full power. But erosion problems have not yet been encountered there, which may partly be due to the fact that Navy ships do not often run at full power for a long time. This indicates that it is not necessarily the bubble cavitation which is erosive, but that some additional properties are required.

One of the reasons that bubble cavitation has a reputation of erosiveness may be its late detection. The amount of nuclei at model scale is nearly always too low and when bubble cavitation is observed at model scale it may have already a significant size at full scale.

A more physical explanation of the erosiveness of bubble cavitation is the location where it normally appears: in the middle of the blade sections at inner radii, as shown in Fig. 5.5. Similar to sheet cavitation this location of cavitation becomes more violent when the propeller operates in a wake. The *dynamic* behavior of bubble cavitation can be such that when the area of bubble cavitation is reducing during a blade revolution, the amount of bubbles collapsing at the same time increases, while the pressure outside the collapsing bubbles increases also. Similar to sheet cavitation this can lead to strong erosion.

These considerations have lead to a reassessment of the erosion danger of bubble cavitation. It seems that steady bubble cavitation as such has no strong erosive properties. It is the dynamic behavior, leading to a collective focussed collapse, which seem responsible for erosion. It is therefore important to observe that on model tests. This requires a proper amount of nuclei.

Bibliography

[1] Arakeri,V.H., Acosta, A.J., 1979, *Viscous Effects in the Inception of Cavitation*, A.S.M.E. Int. Symposium on Cavitation, New York, USA.

[2] Arndt, R.E.A., 1976, *Cavitation on Model Propellers with Boundary Layer Trips*, A.S.M.E.Conference on Polyphase Flow, New Orleans, USA.

[3] Arndt, R.E.A., Ellis, C.R., Paul, S. 1995, *Preliminary Investigation of the Use of Air Injection to mitigate Cavitation Erosion*, A.S.M.E. Journal of Fluids Engineering, Vol.117.

[4] Briggs, L.J., 1950 *Limiting negative pressure of water.*, J. Applied Phys. 21:721722.

[5] Brennen, C.E., 1995 *Cavitation and Bubble Dynamics*, Oxford University Press, ISBN 0-19-509409-3. Also available on internet.

[6] Burrill, L.C., 1951, *Sir Charles Parsons and Cavitation*, Transactions of the Institute of Marine Engineers.

[7] Borkent, B.M., 2009, *Interfacial Phenomena in Micro- and Nanofluidics: nanobubbles,cavitation, and wetting*, Thisis Twente University, The Netherlands.

[8] Coutier-Delgosha, O., Devillers, J-P., Leriche, M., Pichon, T., 2005, emphEffect of Roughness on the Dynamics of Unsteady Cavitation, Journal of Fluids Eng. , vol 127.

[9] Epstein, P.S., Plesset, M.S. 1950 *On the stability of Gas Bubbles in Liquis-Gas Solutions*, Journal of Chemical Physics, Vol.18., pp1505-1509.

[10] , Feindt, E.G., 1956,*Untersuchungen uber die Abhangigkeit des Umschlages Laminar-Turbulent von der Oberflachenrauhigkeit und der Druckverteilung*, Jahrbuch STG, Bd.50, pp180-205

[11] Flynn, H.G., 1964, *Physics of Acoustic Cavitation*, W.P.Mason ed. Vol1,PartB,Academic Press New York-London.

[12] Foeth, E-J., Kuiper, G. 2004, *Exploratory experiments to determine flow and structure borne noise of erosive cavity implosions*, A¿S¿M¿E¿ Fluids Eng. Summer Conference, HT-FED2004-56789, Charlotte, NC. USA.

[13] Foeth, E-J., *The Structure of Three-Dimensional Sheet Cavitation*, Thesis Technical University Delft.

[14] Fox, F.E., Herzfeld, K.F., 1954 *Gas Bubbles with Organic Skin as Cavitation Nuclei*, J.Acoust. Soc. Am. Vol.26, pp 984-989.

[15] Gates, E.M., 1977 *(* The influence of Free-Stream Turbulence, Free Stream Nuclei Populations and a Drag-reducing Polymer on Cavitation Inception on Two Axisymmetric Bodies California Institute of Technology, Rep. No. Eng 183-2.

[16] Harvey, E.N., McElroy, W.D., Whiteley, A.H., 1947 *On Cavity Formation in Water*, Journal of Applied Physics, Vol.18, pp162-172.

[17] Hoekstra, M., Vaz, G. *The Paartial Cavity on a @D Foil Revisited*, 7th Int. Conference on Cavitation CAV2009, Ann Arbor, Michigan, U.S.A.

[18] Holl, J.W., 1960, *An Effect of Air Content on the Occurrence of Cavitation*, Trans. A.S.M.E., Journal of Basic Eng. Vol.82, pp941-946.

[19] Holl, J.W., Carrol, J.A., 1981, *Observations of the Various Types of Limited Cavitation on Axisymmetric Bodies*, PUB A.S.M.E. Journal of Fluids Eng.,Vol 103,pp415-423

[20] Huang, T.T., 1981, *Cavitation Inception Observations on Six Axisymmetric Headforms*, A.S.M.E. Journal of Fluids Engineering, Vol 103,PP273-278

[21] ITTC, 1978,Proceedings 15th ITTC, The Haque, Report of the Performance Committee.

[22] Johnsson, C.A., Hsieh,T., 1966, *The Influence of Trajectories of Gas Nuclei on Cavitation Inception*, 6th Symposium on Naval Hydrodynamics, Washington D.C., pp163-178.

[23] Takagi,K., Kato,H.,Kato,D.,Sugimoto, A., 2006, *Destruction of Plankton by Two-Dimensional Cavitating Jet*, Sixth International Symposium on Cavitation CAV2006, Wageningen, The Netherlands.

[24] Keller, A.P., 1974 *Investigations Concerning Scale Effects of the Inception of Cavitation*, Proc. I.Mech.Eng. Conference on Cavitation, Edinburgh, 109-117.

[25] KLEBANOFF, P.S., SCHUBAUER, G.B., TIDSTROM,K.D., 1955, *Measurements of the Effect of Two-dimensional and Three-dimensional Roughness Elements on Boundary Layer Transition*, J. Aeron. Sciences

[26] Knapp, R.T., Hollander, A., 1948, *Laboratory Investigations of the Mechanism of Cavitation*, Trans. A.S.M.E., Vol.70, pp.419-435.

[27] Knapp, R.T., Daily, J.W., Hammitt, F.G., 1970, *C*avitation, New York : McGraw-Hill.

[28] Knapp, R.T., Hollander, A., 1948, *L*aboratory Investigations of the Mechanism of Cavitation, Trans. A.S.M.E., Vol 70, pp419-435.

[29] Korkut, E., Atlar, M., 2000, *On the Importance of Effect of Turbulence in Cavitation Inception Tests of Marine Propellers*, Proceedings of Royal Society of London A: Mathematical, Physical and Engineering Sciences, Vol.458 , pp.29-48.

[30] Kreider, W., Crum, L., Bailey,M., Matula, T.,Khoklova, V., Sapozhnikov,O., 2006, *Acoustic Cavitation and Medical Ultrasound*,Sixth International Symposium on Cavitation CAV2006, Wageningen, The Netherlands.

[31] Kumar, S., Brennen, C.E., 1996, *A Study of Pressure Pulses generated by Travelling Bubble Cavitation*, Journal of Fluid Mechanics Vol 255 pp541.

[32] Hwansung Lee, Tomonori Tsukiya, Akihiko Homma, Tadayuki Kamimura,Eisuke Tatsumi, Yoshiyuki Taenaka, Hisateru Takano, *Observation of Cavitation in a Mechanical Heart Valve*, Fifth International Symposium on Cavitation (cav2003),Osaka, Japan.

[33] Kuiper, G., 1978, *Scale Effects on Propeller Cavitation*, 12th Symposium on Naval Hydrodynamics, Washington D.C., USA.

[34] Kuiper, G. 1981, *Cavitation Inception on Ship Propeller Models*, Thesis Technical University Delft.

[35] Kuiper, G. 2008, *Fundamentals of Ship Resistance and Propulsion*, Course Lectures Technical University Delft.

[36] Landa, E.R., Nimmo, J.R.,2003 *The Life and Scientific Contributions of Lyman J. Briggs*, Journal of the Soil Science Society of America, Vol 67 no 3, pp 681-693. http://soil.scijournals.org/cgi/reprint/67/3/681

[37] Ligtelijn, J.T., van der Kooij, J., Kuiper, G., van Gent,W., 1992, *Research on Propeller-Hull Interaction in the Depressurized Towing Tank*, Hydrodynamics, Computations,Model Tests and Reality (Marin), Elseviers Science Publishers.

[38] Morch E.M., 2000, Paper on Cav2003.

[39] Moerch, K.A. 2009, *C*avitation Nuclei: Experiment and Theory,Journal of Hydrodynamics Vol21 p176.

[40] Neppiras, E.A., Noltink, B.E., 1951, *Cavitation produced by Ultrasonics*, Proc. Phys. Soc. London, pp 1032-1038.

[41] Ohl, C-D., Arora, M. ,Roy, I., Delius. M., Wolfrum, B.,2003, *Drug Delivery Following Shock Wave Induced Cavitation* , Fifth International Symposium on Cavitation (cav2003),Osaka, Japan.

[42] Plesset, M.S., 1949, *The Dynamics of Cavitation Bubbles*, ASME Journal of Appl. Mech. 1949, pp 277-232.

[43] Schiebe, F.R., 1972, *Measurement of the Cavitation Susceptibility of Water using Standard Bodies*, St. Anthony Fall Hydraulic Lab, Univ. of Minnesota, report 118.

[44] Schlichting, H., 1968, *Boundary Layer Theory*, McGraw-Hill, 6th edition.

[45] Terwisga, T.J.C., Fitzsimmons, P.A., Li,Z., Foeth, E-J. *Cavitation Erosion-A review of Physical Mechanisms and Erosion Risk Models*, 7th International Symposium on Cavitation, CAV2009, Ann Arbor, Michigan, U.S.A.

[46] Jin Wang, 2009, *Nozzle-geometry-dependent breakup of diesel jets by ultrafast x-ray imaging: implication of in-nozzle cavitation*, Seventh Int. Symp. on Cavitation: CAV2009, Ann Arbor, Michigan, U.S.A.

[47] Watanabe, S., Furukawa, A., Yoshida, Y., Tsujimoto, Y., 2009, *Analytical investigations of thermodynamic effect on cavitation characteristics of sheet and tip leakage vortex cavitation*, Seventh Int. Symp. on Cavitation: CAV2009, Ann Arbor, Michigan, USA.

[48] Williams,M., Kawakami, E., Amromin, E., Arndt,R. *Effects of Surface Characteristics on Hydrofoil Cavitation*, Seventh Int. Symp. on Cavitation: CAV2009, Ann Arbor, Michigan, USA.

[49] Yoshimura,T., Kubota, S., Seo, T., Sato,K., 2009, *Development of Ballast Water Treatment Technology by Mechanochemical Cavitations*,Seventh Int. Symp. on Cavitation: CAV2009, Ann Arbor, Michigan, USA.

[50] Yount, D.E. 1979, *S*kins of Varying Permeability: A Stabilization Mechanism For Gas Cavitation Nuclei,A. ACCOUST. SOC. AM. 65(6).

Appendix A

Air Content of Water

The amount of air dissolved in water α can be expressed in many ways. The most common ways in literature are

- the gas fraction in weight ratio α_w
- the gas fraction in volume ratio α_v
- the molecule ratio
- the saturation rate
- the partial pressure of air

A.1 Solubility

Air is a mixture of 21 percent oxygen, 78 percent nitrogen and one percent of many other gases, which are often treated as nitrogen. The specific mass of gases involved in air are:

Oxygen (O_2)	1.429	kg/m^3
Nitrogen (N_2)	1.2506	kg/m^3
Air	1.292	kg/m^3

The maximum amount of gas that can be dissolved in water, the solubility), depends on pressure and temperature. It decreases with increasing temperature and increases with increasing pressure. The solubility of oxygen in water is higher than the solubility of nitrogen. Air dissolved in water contains approximately 36 percent oxygen compared to 21 percent in air.The remaining amount can be considered as Nitrogen. Nuclei which are in equilibrium with saturated water therefore contain 36 percent oxygen. But nuclei which are generated from the air above the water contain 21 percent oxygen. Since the ratio between oxygen and nitrogen is not fixed, it is difficult to relate measurements of dissolved oxygen (by osmose) to measurements of dissolved air (from e.g a van Slijke apparatus).

The amount of oxygen dissolved in water at atmospheric pressure at 15 degrees Celcius is approximately $10 * 10^-6 kg/kg$. For nitrogen this value is about $15 * 10^-6$, so the solubility of air in water is the sum of both: $25 * 10^-6$. Here the dissolved gas contents are expressed as a weigth ratio α_w.Air is very light relative to water and the weight ratio is very small. This ratio is therefore often expressed as parts per million (in weight), which is $10^6 * \alpha_w$.

A.2 The Gas Fraction in Volume Ratio

The volume of gas dissolved per cubic meter of water depends on temperature and pressure. Therefore this volume ratio is expressed in *standard conditions* of 0 degrees Celcius and 1013 mbar (atmospheric conditions). The dependency of the volume of water on temperature and pressure is neglected. The volume of the dissolved air is then described by the law of Boyle-Gay-Lussac:

$$\frac{p * Vol}{273 + T} = constant \tag{A.1}$$

The volume fraction at (p,T) can be related to the volume fraction in standard conditions:

$$\alpha_v = \alpha_v(p, T)\frac{273p}{(273 + T)1013} \tag{A.2}$$

The gas fraction in volume ratio is dimensionless (m^3/m^3). Be careful because sometimes this is violated by using cm^3/l ($1000 * \alpha_v$) or parts per million (ppm) which is $10^6 * \alpha_v$.

α_v is found from α_w by:

$$\alpha_v = \frac{\rho_{water}}{\rho_{air}}\alpha_w \tag{A.3}$$

in which ρ is the specific mass in kg/m^3. At 15 deg. Celcius and 1013 mbar pressure the specific mass of water $\rho_w = 1000kg/m^3$ and the specific mass of air is $1.223kg/m^3$, so for air $\alpha_v = 813\alpha_w$.

A.3 The Gas Fraction in Molecule ratio

The dissolved amount of gas can also be expressed as the ratio in moles(Mol/Mol). Molar masses may be calculated from the atomic weight in combination with the molar mass constant (1 g/mol) so that the molar mass of a gas or fluid in grams is the same as the atomic weight.
The molar ratio α_m is easily found from the weight ratio by

$$\alpha_w = \alpha_m\frac{M_(water)}{M_(gas)} \tag{A.4}$$

in which M is the molar weight, which is 18 for water, 16 for oxygen(O_2) and 28 for Nitrogen (N_2). For air a virtual molar weigth can be defined using the ratio of oxygen and nitrogen of 21/79 this virtual molar weight of air is about 29.

A.4 The saturation rate

The saturation rate is the amount of gas in solution as a fraction of the maximum amount that can go in solution in the same conditions. Since the saturation rate is dimensionless. It is independent of the way in which the dissolved gas or the solubility is expressed. The saturation rate is important because it determines if and in which direction diffusion will occur at a free surface. The saturation rate varies with temperature and pressure, mainly because the solubility of gas changes with these parameters.

A.5 The partial pressure

Sometimes the amount of dissolved gas is expressed as the partial pressure of the gas (mbar or even in mm HG). This is based on Henry's law, which states that the amount of gas dissolved in a fluid is proportional to the partial pressure of that gas. In a van Slijke apparatus a specific volume of water is taken and subjected to repeated spraying in near vacuum conditions (a low pressure decreases the solubility). This will result in collecting the dissolved in a chamber of specific size. By measuring the pressure in that chamber the amount of dissolved gas is found. Note that this pressure is not directly the partial pressure. A calibration factor is required which depends on the apparatus.

Appendix B

Standard Cavitators

A standard cavitator is a reference body which can be used to compare and calibrate cavitation observations and measurements. Its geometry has to be reproduced accurately and therefore an axisymmetric headform has been used as a standard cavitatior.

Such an axisymmetric body has been investigated in the context of the ITTC (International Towing Tank Conference).This is a worldwide conference consisting of towing tanks (and cavitation tunnels) which have the goal of predicting the hydrodynamic behavior of ships. To do that model tests and calculations are used. They meet every three years to discuss the state of the art and to define common problem areas which have to be reviewed by committees. The ITTC headform has a flat nose and an elliptical contour [22]. Its characteristics are given in Fig B.1.

This headform has been used to compare cavitation inception conditions and cavitation patterns in a range of test facilities. The results showed a wide range of inception conditions and also a diversity of cavitation patterns in virtually the same condition, as illustrated in Fig B.3. This comparison lead to the investigation of viscous effects on cavitation and cavitation inception.

The simplest conceivable body to investigate cavitation is the hemispherical headform. This is an axisymmetric body with a hemispere as the leading contour. Its minimum pressure coefficient is -0.74. The hemisperical

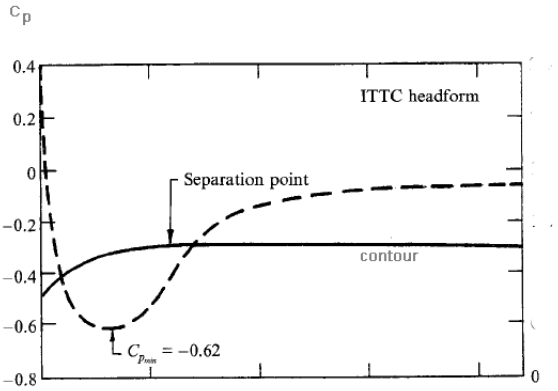

Figure B.1: Contour and Pressure Distribution on the ITTC Headform [31]

headform was used to compare inception measurements in various cavitation tunnels. However, it was realized later on that the boundary layer flow on both the ITTC and on the hemisperical headform was not as simple as the geometry suggested. In most cases the Reynolds numbers in the investigations was such that the boundary layer over the headform remained laminar and the pressure distribution was such that a laminar separation bubble occurred, in the position indicated in Fig. B.1. This caused viscous effects on cavitation inception and made the headform less suitable as a standard body. Note that the location of laminar separation is independent of the Reynolds number. When the Reynolds number becomes high transition to turbulence occurs upstream of the sep-

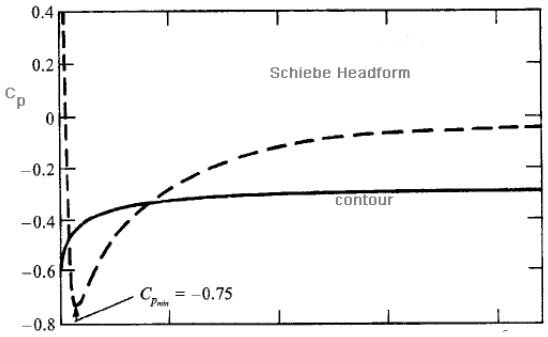

Figure B.2: Contour and Pressure Distribution of the Schiebe body [31]

aration location and separation will disappear.

To avoid laminar separation another headform was developed by Schiebe ([43]) and this headform bears his name ever since. The contour and pressure distribution on the Schiebe headform are given in Fig. B.2. This headform has no laminar separation and transition to a turbulent boundary layer will occur at a location which depends on the Reynolds number.

Many other headform shapes have been investigated with different minimum pressure coefficients and pressure recovery gradients.(e.g.[20])

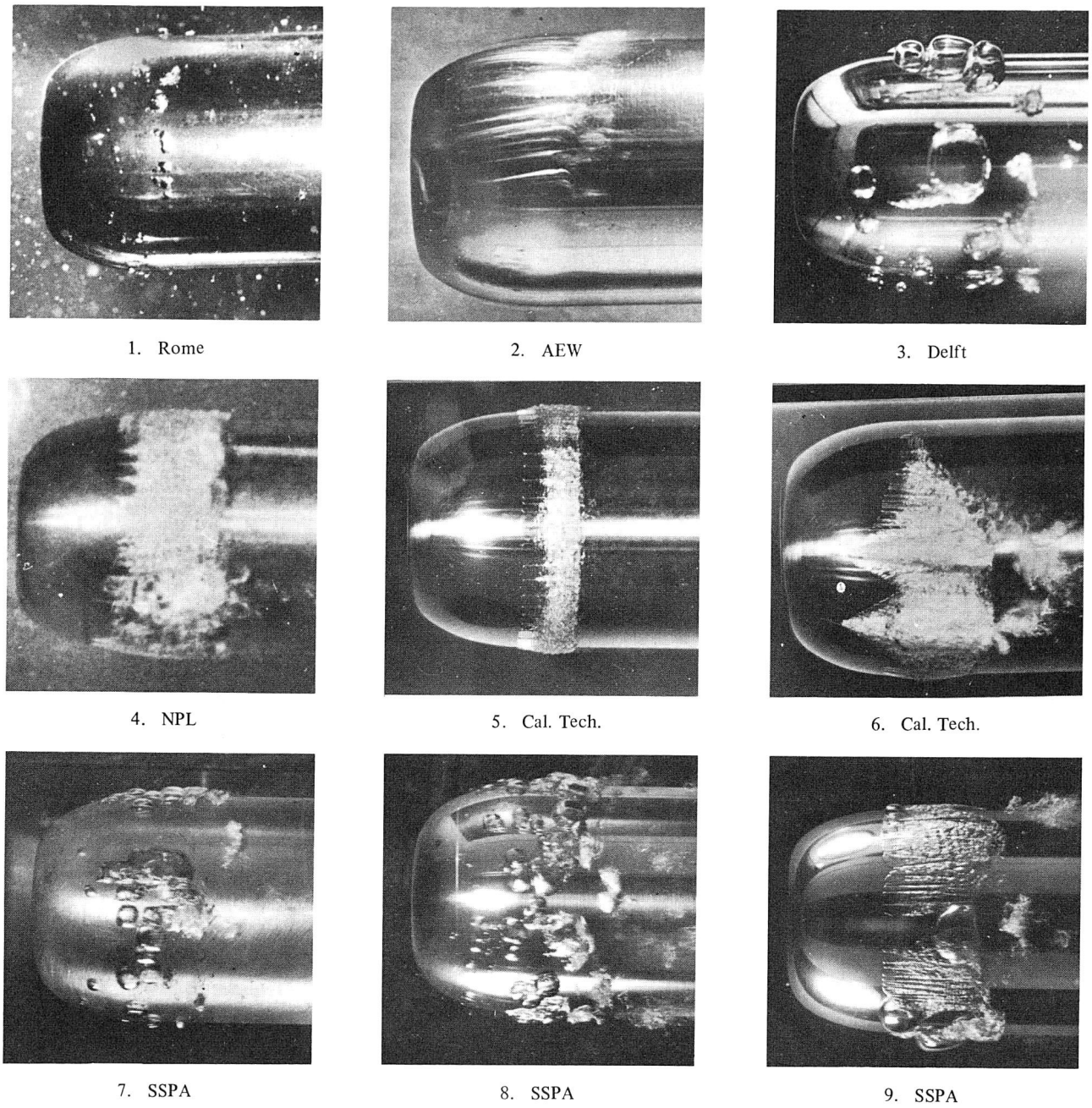

Figure B.3: Comparative measurements of cavitation inception on the ITTC headform source:ITTC

Appendix C

Tables

T Celcius	p_v N/m^2
0	608.012
2	706.078
4	813.951
6	932
8	1069
10	1226
12	1402
14	1598
15	1706
16	1814
18	2059
20	2334
22	2638
24	2981
26	3364
28	3785
30	4236
32	4756
34	5315
36	5943
38	6619
40	7375

Table C.1: Vapor pressure of Water.

Temp. deg. C.	kinem. visc. fresh water $m^2/sec \times 10^6$	kinem. visc. salt water $m^2/sec \times 10^6$
0	1.78667	1.82844
1	1.72701	1.76915
2	1.67040	1.71306
3	1.61665	1.65988
4	1.56557	1.60940
5	1.51698	1.56142
6	1.47070	1.51584
7	1.42667	1.47242
8	1.38471	1.43102
9	1.34463	1.39152
10	1.30641	1.35383
11	1.26988	1.31773
12	1.23495	1.28324
13	1.20159	1.25028
14	1.16964	1.21862
15	1.13902	1.18831
16	1.10966	1.15916
17	1.08155	1.13125
18	1.05456	1.10438
19	1.02865	1.07854
20	1.00374	1.05372
21	0.97984	1.02981
22	0.95682	1.00678
23	0.93471	0.98457
24	0.91340	0.96315
25	0.89292	0.94252
26	0.87313	0.92255
27	0.85409	0.90331
28	0.83572	0.88470
29	0.81798	0.86671
30	0.80091	0.84931

Table C.2: Kinematic viscosities adopted by the ITTC in 1963

R_n	$C_f \times 10^3$
1×10^5	8.333
2	6.882
3	6.203
4	5.780
5	5.482
6	5.254
7	5.073
8	4.923
9	4.797
1×10^6	4.688
2	4.054
3	3.741
4	3.541
5	3.397
6	3.285
7	3.195
8	3.120
9	3.056
1×10^7	3.000
2	2.669
4	2.390
6	2.246
8	2.162
1×10^8	2.083
2	1.889
4	1.721
6	1.632
8	1.574
1×10^9	1.531
2	1.407
4	1.298
6	1.240
8	1.201
1×10^{10}	1.17x

Table C.3: Friction coefficients according to the ITTC57extrapolator.

Temp. deg. C.	density fresh water kg/m^3	density salt water kg/m^3
0	999.8	1028.0
1	999.8	1027.9
2	999.9	1027.8
3	999.9	1027.8
4	999.9	1027.7
5	999.9	1027.6
6	999.9	1027.4
7	999.8	1027.3
8	999.8	1027.1
9	999.7	1027.0
10	999.6	1026.9
11	999.5	1026.7
12	999.4	1026.6
13	999.3	1026.3
14	999.1	1026.1
15	999.0	1025.9
16	998.9	1025.7
17	998.7	1025.4
18	998.5	1025.2
19	998.3	1025.0
20	998.1	1024.7
21	997.9	1024.4
22	997.7	1024.1
23	997.4	1023.8
24	997.2	1023.5
25	996.9	1023.2
26	996.7	1022.9
27	996.4	1022.6
28	996.2	1022.3
29	995.9	1022.0
30	995.6	1021.7

Table C.4: Densities as adopted by the ITTC in 1963.

Appendix D

Nomenclature

ρ	density of water	$\frac{kg}{m^3}$	See TableC.4
C_g	gas concentration	kg/m^3	see Appendix A
D_g	diffusion coefficient	m^2/sec	representative value $2 * 10_9$
D	diameter	m	
F_d	drag	N	
g	acceleration due to gravity	$\frac{m}{sec^2}$	Taken as 9.81
Nd	number density of nuclei	m^-4	
p_g	gas pressure	$fracNm^2$	
$fracNm^2$			
p_v	equilibrium vapor pressure		
R	radius	m	
μ	dynamic viscosity of water	$\frac{kg}{m*sec}$	
ν	kinematic viscosity of water	$\frac{m^2}{sec}$	$(\nu = \frac{\mu}{\rho})$See Table C.2
s	surface tension	Nm	for water 0.075